Simulation of tau decays, ambiguities and anomalous couplings effects

Jim John, **Ananya Tapadar**, Zbigniew Was

Institute of Nuclear Physics, IFJ-PAN, Radzikowskiego 152, 31-342 Krakow, Poland

Cracow School of Theoretical Physics

Polish Academy of Arts and Sciences, 17 Sławkowska str., Kraków.

19/06/2025

Outline

- Introduction

- Our code: application external to KKMCee (see website: : https://th.ifj.edu.pl/kkmc-demos/index.html) for separating Hard interaction from ISR, only.

    1. **Check:** Sanity check and factorization checks (scattering angle).
    2. **Applications:** a) Measurement of Weinberg angle (Helicity attribution)

        b) Search for new physics (Polarimetric vectors) (I do not understand this)

- Conclusion

Introduction:

- KKMC is high-precision generator for $e^+e^- \to f\bar{f}$ processes and includes both **initial-state radiation (ISR)** and **final-state radiation (FSR) and interference**.

- In response to requests from experimental collaborations, over the past few months, we have focused on two specific topics:

  a) development of helicity-like flags to measure the Weinberg angle.
  b) prepare the use of polarimetric vectors to implement potential new-physics effects.

- The idea is to manipulate information from matrix elements into quantities useful for practical applications.

  I shall cover two: a) helicity-like flags for tau lepton spin correlation

  b) polarimetric vectors for tau lepton decays.

New attributes and motivation :

- We have added new attributes to the 'hepmc3' output from the **C++** version of **KKMCee**:

1. Tau helicity-like flags to separate samples for fits, like it was done in $\frac{g_V}{g_A}$ measurements at LEP .

   New modes are introduced: 1. Chiral mode: where the projection of Polarimetric vectors is taken along the momentum of tau.

   2. Internal mode: where the projection of the **Polarimetric vectors** is taken along the internal z-axis of KKMC.

   COMMENT: They coincide in $\frac{m_\tau}{E} \to 0$ limit.

2. Polarimetric vectors of tau in the lab frame (polarimetricInLabFrame) to enable introduction of new physics interaction in the tau production+decay on top of the standard QED corrected simulation, no compromising precision like in [*Phys.Rev.D 106 (2022) 11, 113010; SB, AYK, ZW*]

   COMMENT: For NP, only simplified 2 to 2 kinematics is expected to be used (with its frame orientations).

- Application of (1) was used in the precise measurement of the Weinberg Angle already by ALEPH collaboration *[Eur.Phys.J.C20:401-430,2001]* but now in C++ with better SM and more flexibility.

- Application of (2) for anomalous tau dipole moments already available in **f77**, but in a less user-friendly way than now *[Phys.Rev.D 109 (2024) 1, 013002; SB, AYK, ERW, ZW].*

- Current version of KKMCee is available at https://holeczek.web.cern.ch/public/KrakowHEPSoft/KKMCee-dev/

Preparation of application external to KKMCee:

- Our ongoing work includes to learn and understanding the phenomenology of QED. That includes looking at factorizations.

  1) KKMC has a second-order QED matrix element included and offers perfect implementation.

  2) New Physics effects, we may want to use a simpler picture. Essentially, of factorization type: into Born-like configurations and bremsstrahlung part (at present, we consider initial state radiation only).

ADVANTAGE: The user does not need to know the technicalities and details of frame orientations of KKMCee. User need to worry about their own choice of reference frames only, and ensure their relation to the lab frame.

- For now, two choices of reference frames are used in the application:
  a) Colins-Soper frame b) Mustraal frame

- Details of frame orientations must be connected with those of KKMCee, because we need to take care of properties of tau decays (polarimetric vectors).

We will cover some results/exercises in the following slides.

Sanity & factorization checks: Scattering angle

- KKMC has it better, so with it we can check how factorized Born kinematic works.
- In the presence of the ISR, the Mustraal frame matches better with the theoretical prediction.

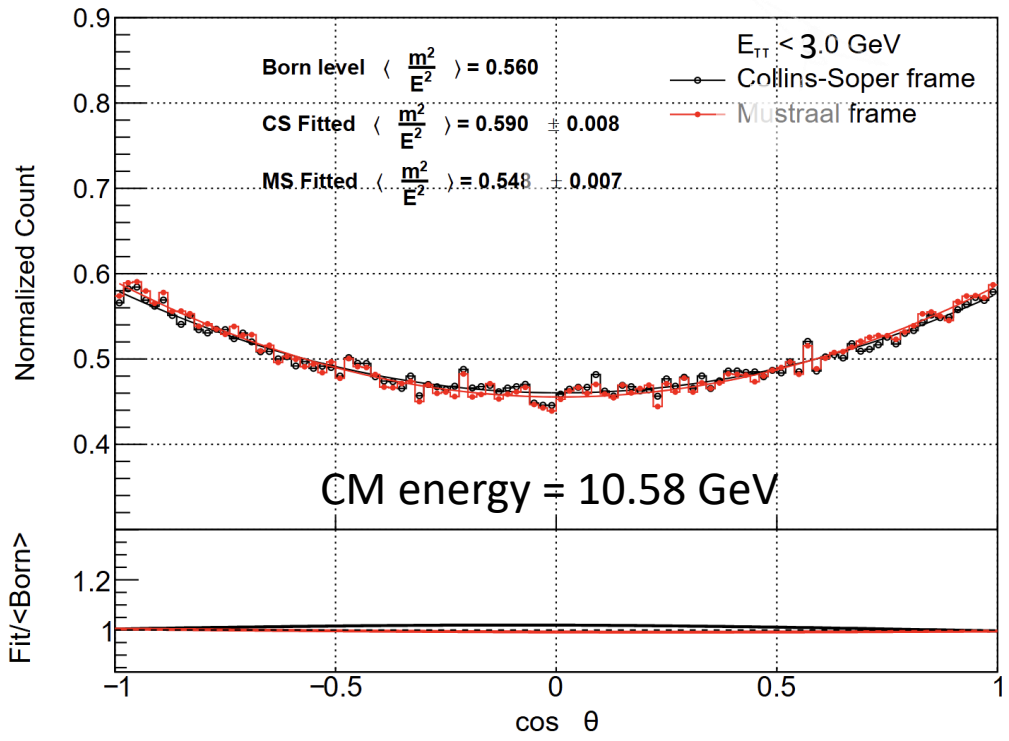

The plots are made with 10 million events and statistical error is not evaluated.

$$\frac{d\sigma^{\langle \mathrm{Born}\rangle}}{d\cos\theta} = 1+\cos^2\theta+\langle\frac{m_\tau^2}{E^2}\rangle \sin^2\theta+\frac{3}{8}\langle A_{\mathrm{FB}}\rangle \cos\theta$$

$$\mathrm{fmodel} = 1+\cos^2\theta_{\mathrm{CS}} + F_1 \sin^2\theta_{\mathrm{CS}} + F_2 \cos\theta_{\mathrm{CS}}$$

$$\mathrm{fmodel} = 1+\cos^2\theta_{\mathrm{M}} + F_1 \sin^2\theta_{\mathrm{M}} + F_2 \cos\theta_{\mathrm{M}}$$

$E_{\tau\tau} =$ Invariant mass of tau pair system/2.

We effectively sum contributions of Born from different energies, that is why $\langle\frac{m_\tau^2}{E^2}\rangle$ and $\langle A_{\mathrm{FB}}\rangle$ are averaged.

How well is it reproduced? We use plots to evaluate. <…> means averaging with the photon spectrum as KKMCee generated.

CM energy = 10.58 GeV

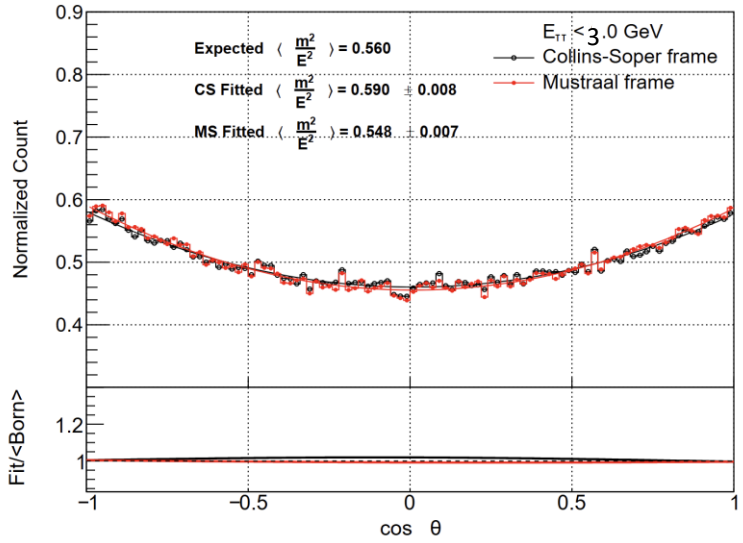

The Collins-Soper frame is constructed for LO, no radiative corrections are built into the coordinate system.

Mustraal algorithm to reconstruct the event's effective "Born-like" reference frame after photon emission (NLO).

CM energy = 74.06 GeV

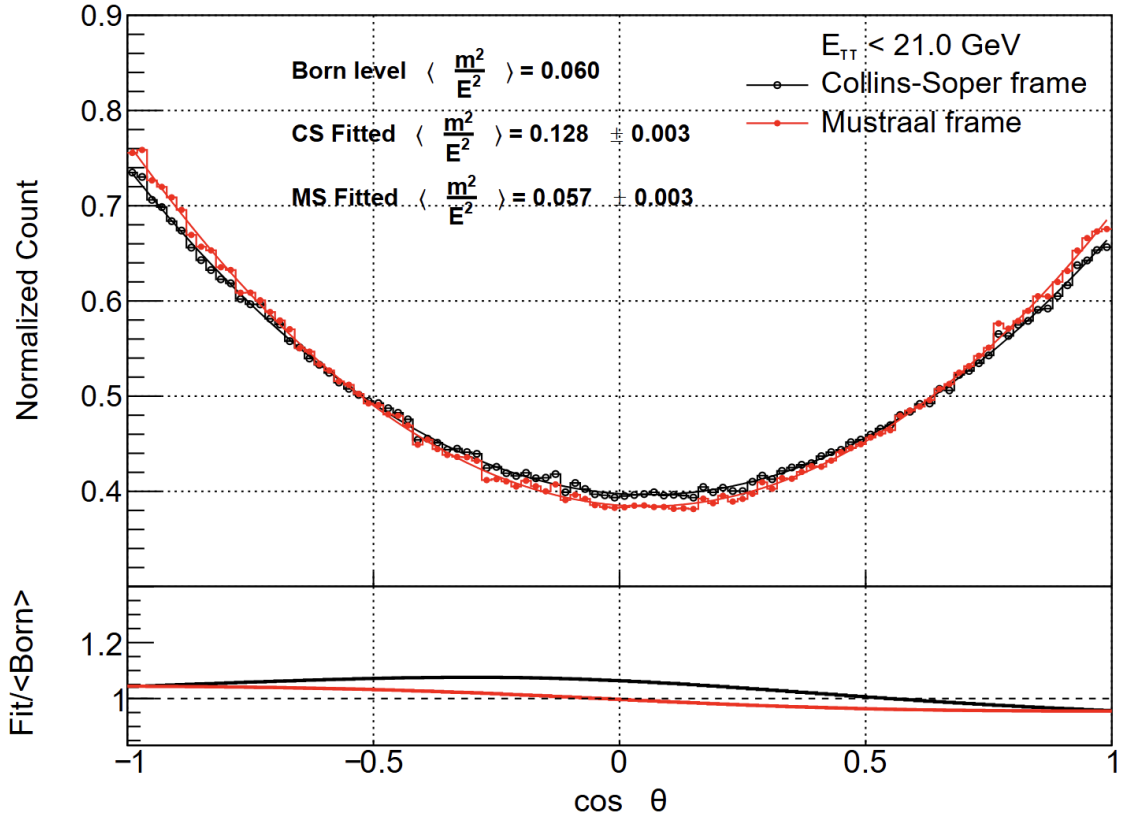

CM energy = 10.58 GeV

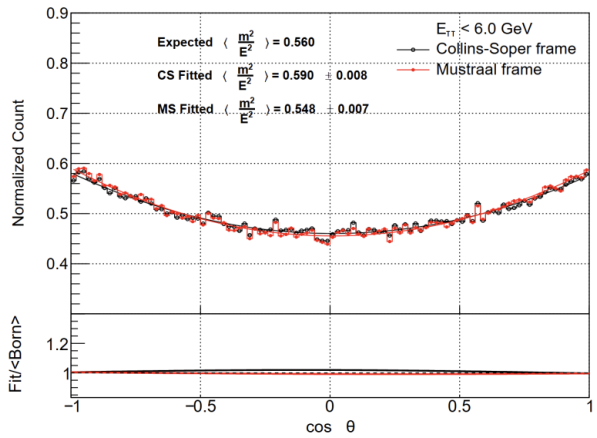

To be fixed: mismatch of the ratio plots from KKMC and the application still need to be fixed.

CM energy = 42.32 GeV

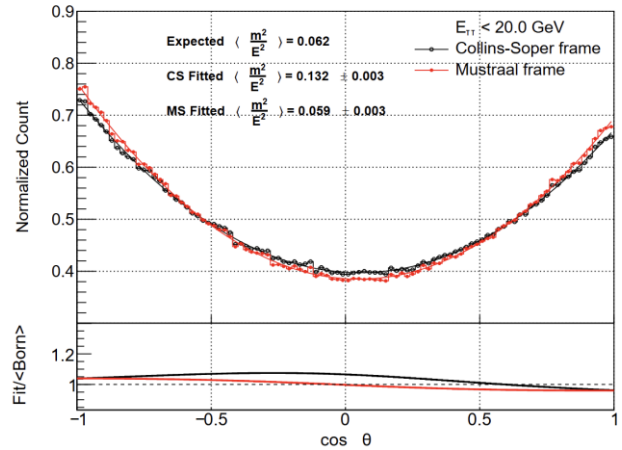

CM energy = 91.17 GeV

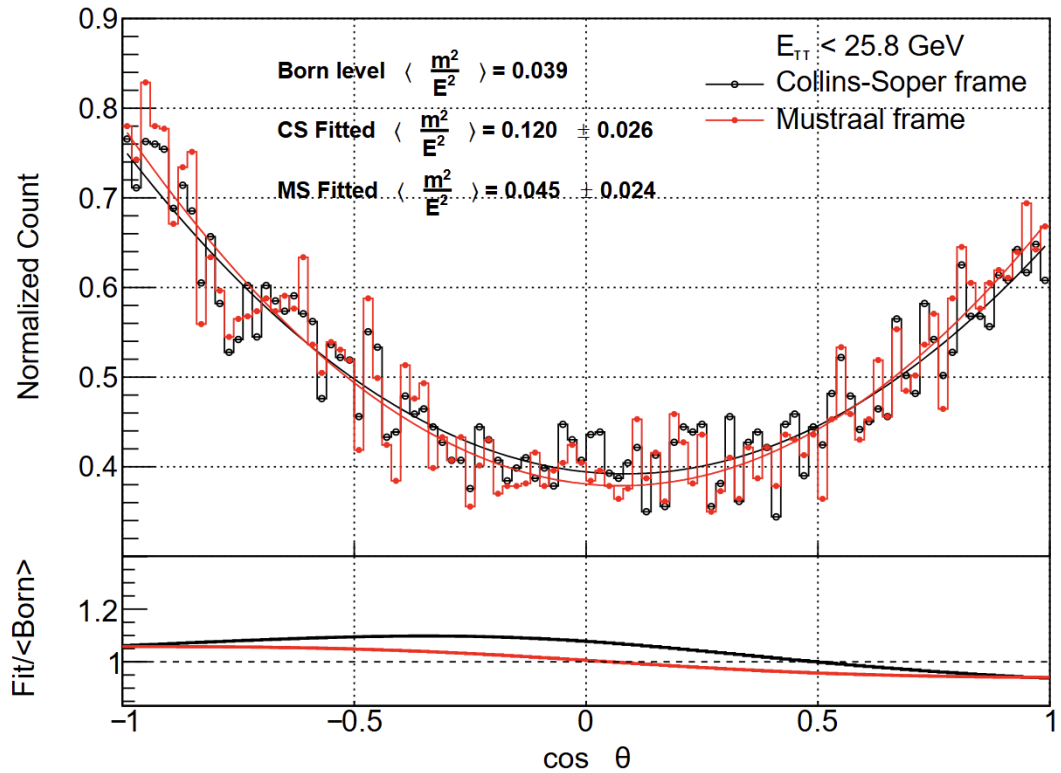

Conclusion for the part:

- Separation into Born-like variables and photon emission part works sufficiently well for our application, which is to modify small-scale interactions. That is a Born level (partial) differential distribution.
  - ✓ True for Collins-Soper, which is conceptually improved leading log(LL).
  - ✓ True for the Mustraal frame, which takes into account QED single emission matrix element properties (NLL).
  - ✓ We need more effort on parameter tuning.

In the following slides, we move to the next subject:

- Helicity attribution has already been used in the ALEPH $\frac{g_V}{g_A}$ measurement.
- Some tests and plots describing details (for this type of production/decay factorization)
- Evaluation of ambiguities.

Looking and validating the helicity approximation:

- We looked into the helicity approximated weight. We introduced this by introducing the outer product of two vectors of pure spin state + means (1, 0, 0, 1) and – means (1, 0, 0, -1), $\mathbf{p}_\tau$ along z-axis.

Rewrite approximated weight : $$wt = \sum_{i,j=t,z} h_i^{\tau^+} R_{ij} h_j^{\tau^-} \longrightarrow wt = \sum_{m,n=\pm} h_m^{\tau^+} R_{mn} h_n^{\tau^-}$$

- The introduction of these vectors helped us to present the approximated spin weight in the helicity/chiral states contribution; transverse degrees of freedom were dropped earlier.

- In the case of the CHIRALITY mode, we project polarimetric vectors along the momentum of tau.

- This approach was used for precise measurement of Weinberg angle from Tau decays already in earlier times e.g. in ALEPH collaboration.

People want to have Helicities for decaying taus: Impossible (quantum entanglement) without approx.

- In our (KKMCee external) code, tau momenta are along the momentum of tau.

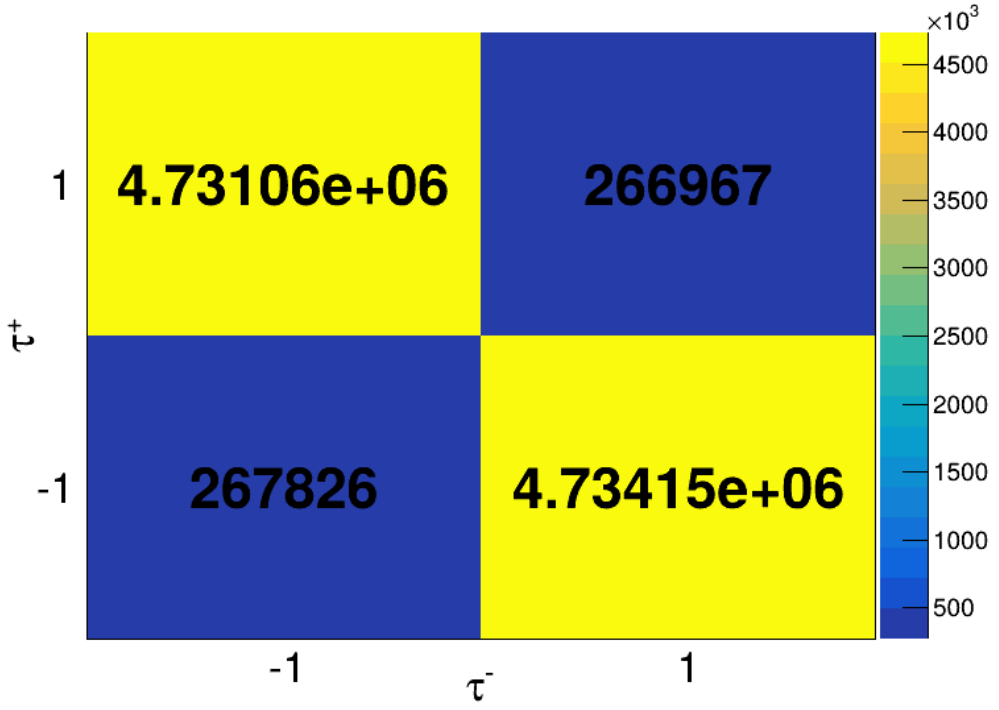

CM energy = 10.58 GeV

- First plot on helicity-like attributed

-+ ++

-- +-

- This is 10.58 GeV CMS energy and most events are in Yellow (-+, +-) boxes.

- Plot is done at Born level, no Bremsstrahlung KKMCee internal variables.

- No ambiguities in the choice of the momentum direction.

Note! KKMCee has its own way of choosing z direction, also in the case of Brem. Massive smearing of z direction (adaptation to Kleiss-Stirling techniques). **We use momentum direction New:** tralo4(-1/-2,….).

Helicity-like distribution (Plots are nearly same):

- In our code, tau momenta are projected along the z-axis.

Our code

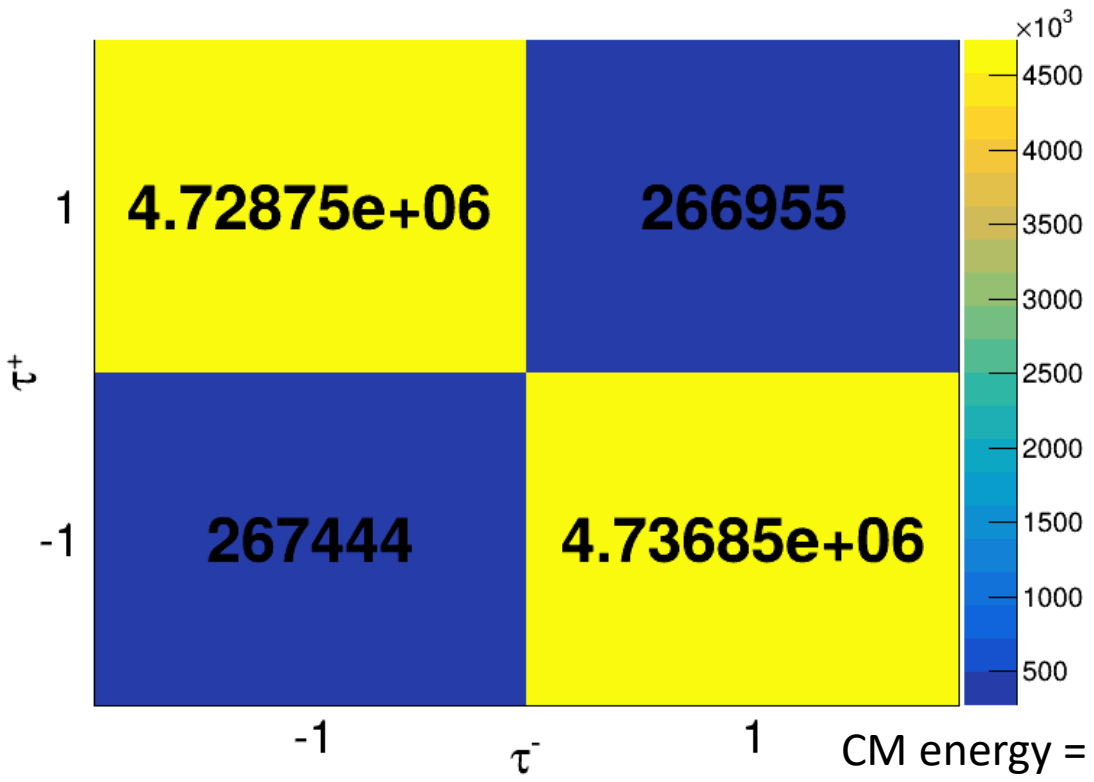

KKMCee along tau momentum

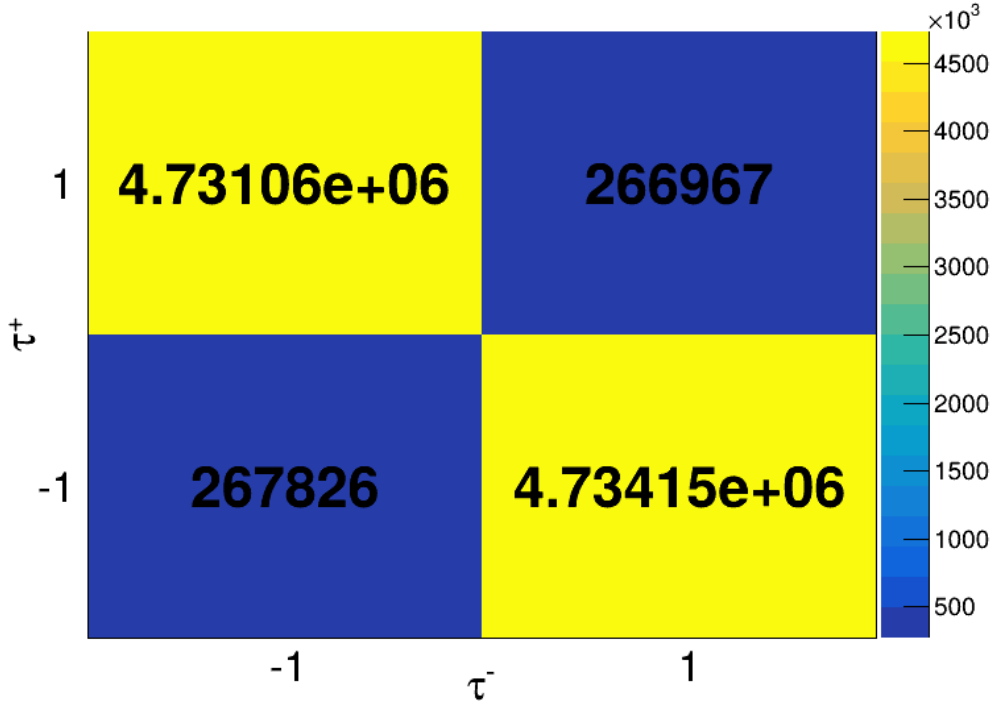

CM energy = 10.58 GeV

Table: Helicity fractions at 10.58 GeV without ISR (Mustraal frame)

The Mustraal frame removes residual ISR impact ; results shown for the momentum direction basis.

10.58 GeV	-+	--	++	+-
$\|\cos\theta\| < 0.05$ KKMCee	0.449303	0.0506367	0.051651	0.44841
$\|\cos\theta\| < 0.05$ External	0.449382	0.0504906	0.0509282	0.44920

10.58 GeV	-+	--	++	+-
$\|\cos\theta\| > 0.98$ KKMCee	0.499347	0.000616892	0.000470692	0.499565
$\|\cos\theta\| > 0.98$ External	0.499183	0.00060976	0.000602629	0.499604

Observation from the tables:

1. **Numerical agreement:** KKMCee and the external calculation agree within 10^{-3}, confirming consistent helicity reconstruction (statistical error is not checked yet).

2. **Photon-dominated regime:** At 10.58 GeV, the process is purely QED; opposite-helicity ($\tau_R^- \tau_L^+$ and $\tau_L^- \tau_R^+$, L and R is for **chirality**) components dominate equally, indicating negligible Z-exchange or parity-violating effects.

3. **Central vs. forward behaviour:**
   a) In the **central region** ($|\cos\theta| < 0.05$), small but visible helicity-flip components appear ($\propto m^2/s$).
   b) In the **forward region** ($|\cos\theta| > 0.98$), helicity is almost perfectly conserved; flip terms are $< 10^{-3}$.

Conclusion from the tables:

The helicity reconstruction is validated at 10.58 GeV: the results agree with KKMCee within 0.001 %. The distributions exhibit the expected QED pattern—helicity conservation in the forward/backward regions and small mass-suppressed flips near 90°. This confirms that the Mustraal frame and spin-density reconstruction are functioning correctly.

Table: Helicity fractions at 42.32 GeV without ISR (Mustraal frame)

The Mustraal frame removes residual ISR boosts; results shown in the momentum direction basis.

42.32 GeV	-+	--	++	+-
$\|\cos\theta\| < 0.05$ KKMCee	0.490986	0.00364181	0.00341619	0.501956
$\|\cos\theta\| < 0.05$ External	0.490617	0.00334186	0.00338168	0.50266

42.32 GeV	-+	--	++	+-
$\|\cos\theta\| > 0.98$ KKMCee	0.494895	0.0000338524	0.0000440081	0.505027
$\|\cos\theta\| > 0.98$ External	0.495345	0.0000372376	0.0000203114	0.504597

Observation from the tables:

1. **Helicity-flipped events decrease further** with the increase of energy, as expected from the $\frac{m_\tau^2}{s}$ suppression.

2. **An asymmetry between the −+ and +− components** now appears at 42 GeV, while they were equal at 10.58 GeV. This indicates the **onset of photon–Z boson interference.**

3. **Below the Z pole, the interference term gives a negative contribution.**
   The Z propagator denominator $\left(s - M_Z^2\right)$ is negative at 42 GeV, so the γ–Z interference is **destructive.**

$$\sigma_{-+} < \sigma_{+-}$$

Conclusion from the tables:

1. The difference between σ_{-+} and σ_{+-} directly signals the γ–Z interference effect.

2. The smaller value of R_{-+} below the Z pole confirms that the interference term contributes **negatively**, consistent with the expected sign of the Z propagator.

Table: Helicity fractions at 42.32 GeV without ISR (Mustraal frame)

The Mustraal frame removes residual ISR boosts; results shown in the momentum direction basis.

1. At low energies ($E \simeq$ Z boson mass)

91.17 GeV	-+	--	++	+-
$\|\cos\theta\| <$ 0.05 KKMCee	0.571927	0.0000106361	0.00000797707	0.428055
$\|\cos\theta\| <$ 0.05 External	0.573317	0.0000132951	0.00000531805	0.426664

91.17GeV	-+	--	++	+-
$\|\cos\theta\| > 0.98$ KKMCee	0.573248	0.0000134915	0.0000101186	0.426728
$\|\cos\theta\| > 0.98$ External	0.575414	0.0001437 33	0.0001300 44	0.424586

Observation from the tables:

1. **At the Z pole, the interaction is dominated by Z exchange.** The photon contribution becomes small, and helicity-flip channels are reduced to the 10^{-6} level.

2. **A strong left–right asymmetry appears:**
   $R_{LL} \sim 0.57 > R_{RR} \sim 0.43,$ L, R denotes chirality
   This reflects the **chiral structure of the Z couplings**, where $g_L > g_R$,so left-handed $\tau^-\tau^+$ pairs are produced more often than right-handed ones.

3. **At** $s = M_Z^2$ the γ–Z interference term **changes sign** (since the propagator $s - M_Z^2 \approx 0$(so the previously negative interference seen below the pole **vanishes** here).
   The remaining asymmetry now arises purely from the intrinsic **Z-boson parity violation.**

Conclusion from the tables:

1. At the Z resonance, production is almost entirely through the Z boson.
   The helicity pattern $R_{LL} > R_{RR}$ confirms the dominance of the left-handed coupling g_L.
2. Photon–Z interference is minimal at this energy and changes sign as the beam energy crosses the pole.

Table: Helicity fractions at 10.58 GeV with ISR & FSR

10.58 GeV	-+	--	++	+-
$\|\cos\theta\| < 0.05$ KKMCee	0.4306520887	0.0686753332	0.0676096901	0.4330628879
$\|\cos\theta\| < 0.05$ External	0.4369411301	0.0624911092	0.0619819964	0.4385857643

10.58 GeV	-+	--	++	+-
$\|\cos\theta\| > 0.98$ KKMCee	0.499347	0.000616892	0.000470692	0.499565
$\|\cos\theta\| > 0.98$ External	0.499183	0.00060976	0.000602629	0.499604

Observation from the tables:

1. **Numerical agreement! :** KKMCee and the external calculation agree within 10^{-2}.

2. **ISR–FSR effects at 10 GeV:**
   Both ISR and FSR were included in the simulation. At low energy, the radiation pattern is **dominated by ISR**,
   $$\ln\left(\frac{s}{m_e^2}\right) \gg \ln\left(\frac{s}{m_\tau^2}\right)$$

3. The helicity-flip components (**––**, **++**) show a slight increase compared to the pure Born-level case. This behaviour reflects **mass-suppressed longitudinal contributions** that become visible when both **ISR and FSR** are included.

Conclusion from the tables:

1. Small FSR is as expected out of the application frame.

Table: Helicity fractions at 42.32 GeV with ISR & FSR

42.32 GeV	-+	--	++	+-
$\|\cos\theta\| < 0.05$ KKMCee	0.4694788075	0.0254772268	0.0252484283	0.4797955374
$\|\cos\theta\| < 0.05$ External	0.4787971442	0.0155322944	0.0154100952	0.4902604662

42.32 GeV	-+	--	++	+-
$\|\cos\theta\| > 0.98$ KKMCee	0.4712674997	0.0230432548	0.0232812408	0.4824080046
$\|\cos\theta\| > 0.98$ External	0.4940555232	0.0001379629	0.0001345138	0.505672001

Observation from the tables:

1. The overall mismatch between **KKMCee** and the **external code** increases slightly, particularly in the forward region.
2. This trend is expected since **FSR** becomes relatively more important with energy, and photon emission from the final τ's depends sensitively on the spin-recoil treatment.
3. The small helicity-flip components (––, ++) are most affected, while the main helicity-conserving channels remain consistent within a few percent.

Conclusion from the tables:

1. At **42.32 GeV**, the agreement between **KKMCee** and the **external reconstruction** remains good overall but shows slightly larger deviations than at 10.58 GeV, especially in the forward region.

Table: Helicity fractions at 91.17 GeV with ISR & FSR

91.17 GeV	-+	--	++	+-
$\|\cos\theta\| <$ 0.05 KKMCee	0.5697648634	0.0000106361	0.0000079770 7	0.4293267574
$\|\cos\theta\| <$ 0.05 External	0.5707400352	0.0000774794	0.0000961813	0.4290863 04

91.17GeV	-+	--	++	+-
$\|\cos\theta\| > 0.98$ KKMCee	0.5708947786	0.0001250021	0.0000945962	0.4288856231
$\|\cos\theta\| > 0.98$ External	0.5716110069	0.0	0.0	0.4283889931

Observation from the tables:

1. At **91 GeV**, the helicity pattern is now fully dominated by **Z- boson exchange**, and both codes show **excellent agreement**—within **0.1 %** for the main helicity channels (−+, +−).

2. The **(−−)** and **(++)** components are extremely suppressed ($\sim 10^{-4}$), consistent with the **mass-suppressed longitudinal contributions** expected at the Z pole.

3. The **γ–Z interference** term vanishes here because the Z propagator is purely imaginary at s = M_Z^2, so the asymmetry arises entirely from the chiral structure of the Z couplings (v ± a).

Conclusion from the tables:

1. Near the Z mass, both **KKMCee** and the **external reconstruction** reproduces the pure-Z behaviour with sub-per-mille precision.
2. The helicity-flip terms remain negligible, confirming that **longitudinal and interference effects are strongly suppressed** at the resonance.
3. The result validates the consistency of the spin-density reconstruction in the **Z-dominated regime**, where parity-violating effects fix the asymmetry purely through the Z couplings.

Application: A. ALEPH comparison,

1. Since the external reconstruction reproduces the **KKMCee helicity fractions** with sub-per-mille accuracy at the **Z pole**, it can now be confidently used to **assign helicity states event-by-event**, following the same strategy adopted by the **ALEPH Collaboration**.

2. In particular, the validated external algorithm can serve as an independent **helicity attribution tool**, allowing experimental analyses to extract **τ polarization and spin-correlation observables** directly from generated or reconstructed data, without relying on internal KKMC routines.

3. Application can attribute helicities for muons as well (Request for this has arisen).

Application: B. New Physics,

In the next part, we focus on Polarimetric vectors and its application to new physics searches.

τ four-momenta (p_{τ^-}, p_{τ^+} to define spin quantization axes)

τ rest frames (to compute polarimetric vectors h^{μ}).

Polarimetric Vectors and Spin Correlations

1. **τ leptons are polarized** in their production (e.g. from Z/γ* exchange).
   This polarisation influences how their decay products are distributed.

2. Each τ decay responds to the spin state through the **polarimetric vector** h^{μ}.

3. For a τ pair, spin–spin correlations appear as:

$$d\sigma = \sum_{i,j=1,4} h_i^{\tau^-} R_{ij} h_j^{\tau^+}$$

4. τ rest frames cannot be reconstructed experimentally because of **missing neutrinos**.

5. The **ρρ system** is fully visible; its rest frame preserves the relative decay-plane geometry, and the spin state of the tau is correlated with the spin state of its decay product, ρ.

6. The **acoplanarity angle (ϕ*)**, defined as the angle between the two ρ decays, oriented half-planes, in the ρρ rest frame. Acts as an *effective observable* of transverse spin correlations.

- The **acoplanarity angle (ϕ*)** is the relative azimuthal angle between these two planes, measured in the **ρρ rest frame**:

$$\hat{n}_{\pm} = \frac{\vec{p}_{\pi_{\pm}} \times \vec{p}_{\pi^0}}{|\vec{p}_{\pi_{\pm}} \times \vec{p}_{\pi^0}|}$$

- The acoplanarity angle ϕ* probes the **transverse spin–spin correlations** of the τ pair.
  It originates from the interference between opposite-helicity amplitudes.

- Introduction to NP (dipole moments : a(s) magnetic and b(s) electric):

$$\Gamma^{\mu} = \gamma^{\mu} + \frac{\sigma^{\mu\nu} q_{\nu}}{2m} \left[ia(s) + \gamma_5 b(s)\right]$$

- Any deviation from SM distribution — such as a phase shift or modulation — could signal contributions from dipole operators $a(s)$or $b(s)$.

- QED contribution to the first order in fine structure has been explicitly included in our code.
- Spin reweighting technique : $wt = \left(\frac{\sigma(s, \cos\theta)^{\mathrm{SM+NP}}}{\sigma(s, \cos\theta)^{\mathrm{SM}}} \right)$

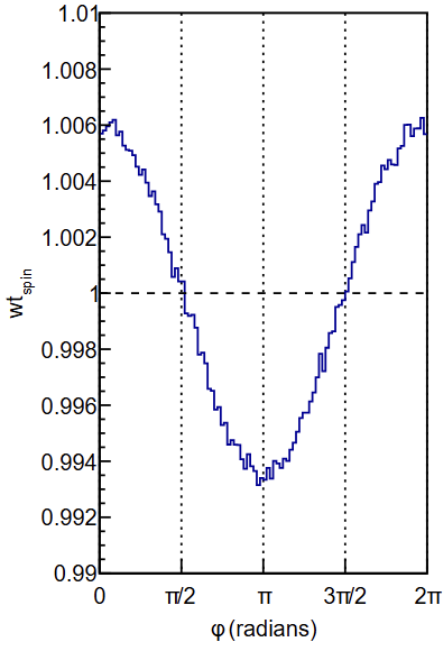

$\mathrm{Re}(a) = 0.04,$

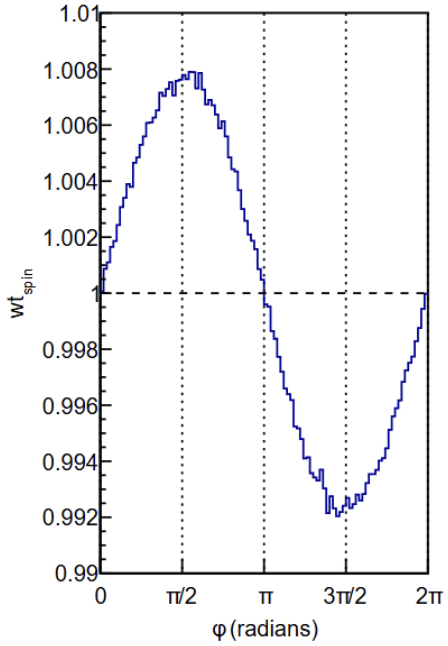

$\mathrm{Re}(b) = 0.04,$

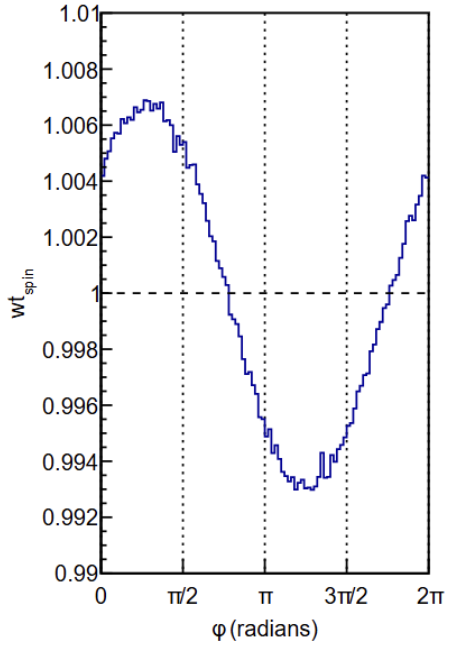

$\mathrm{Re}(a\_\{NP\}) = 0.04 \cos\left(\frac{\pi}{4}\right)$

$\mathrm{Re}(b\_\{NP\}) = 0.04 \sin\left(\frac{\pi}{4}\right)$

Observation from the Plots:

1. It is seen from these figures that the effect of the anomalous couplings on the distribution can reach about 0.005 (depends on parameters value).

2. Algorithm is prepared to work independently of KKMC Monte Carlo.

3. ϕ* analysis accesses τ transverse spin correlation, and it is independent of neutrino reconstruction.

4. WE reconstruct plots from [PhysRevD.106.113010, Sw. Banerjee , A.Yu. Korchin , and Z. Was].

- Energy cuts : $y_- = \frac{E_{\pi^-} - E_{\pi^0}}{E_{\pi^-} + E_{\pi^0}}$ $y_+ = \frac{E_{\pi^+} - E_{\pi^0}}{E_{\pi^+} + E_{\pi^0}}$

Take away:

1. **Helicity attribution** gives the initial spin state (longitudinal polarization).
2. It is possible to assign **helicity-like** attribution **event-by-event**, reproducing the ALEPH strategy at the Z pole.
3. **Polarimetric vectors** describe the response of decay to that spin.
4. **Acoplanarity (ϕ*)** isolates the *transverse spin effects, which are beyond the helicity picture.*
5. **New Physics** introduces complex phases altering ϕ* modulation.

Our code demonstrates consistent behaviour across both longitudinal and transverse components, yielding physically reliable results over a wide range of energy scales up to some precision. However, further refinement is required to improve the precision.

Current version and future updates of our code is available at : https://th.ifj.edu.pl/kkmc-demos/index.html

The same technique of phase space ME manipulations was used for PHOTOS to generate dark photons or light scalars (not by me in f77, but now also in C++, which is my work) .

Acknowledgement: The project was supported in part from funds of the National Science Centre, Poland, grant no. 2023/50/A/ST2/00224 and of COPIN-IN2P3 collaboration with LAPP-Annecy.

Improvements:

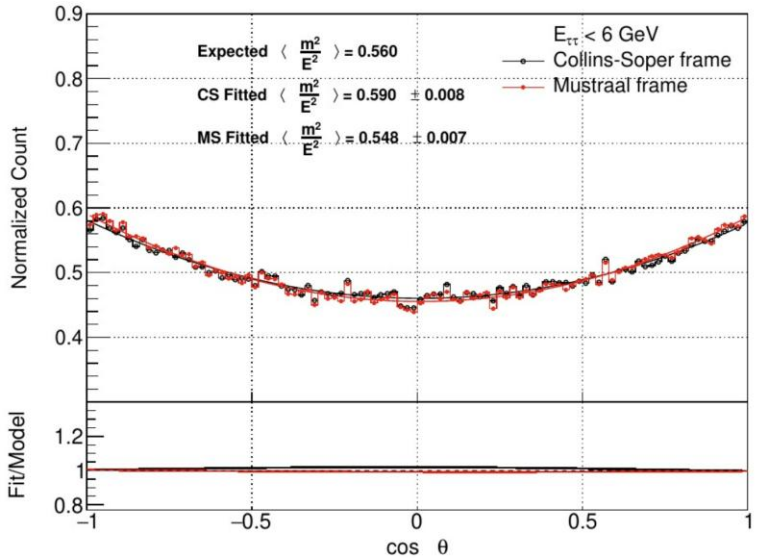

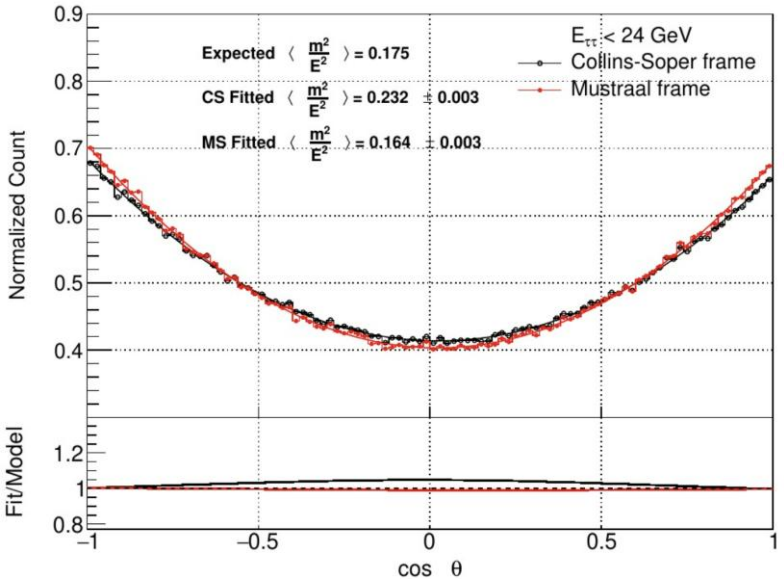

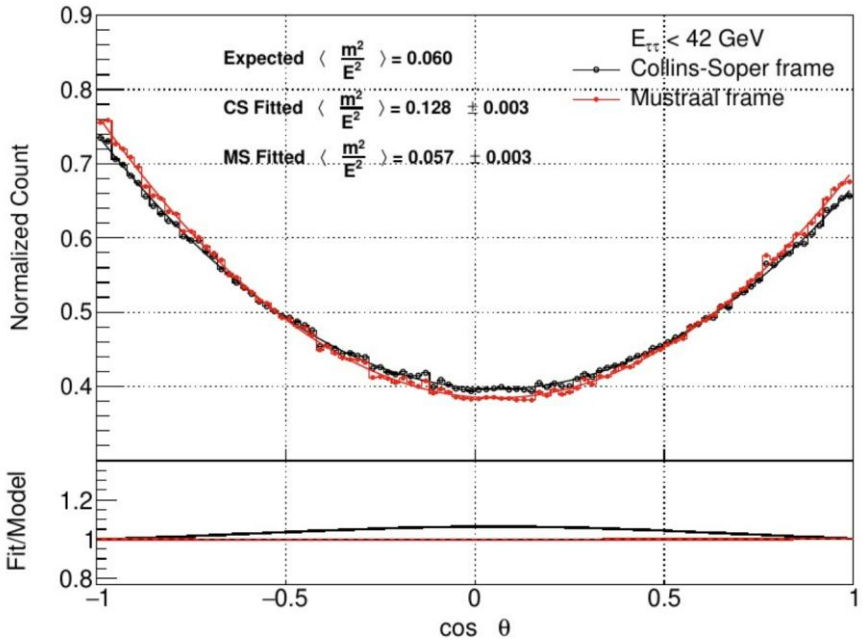

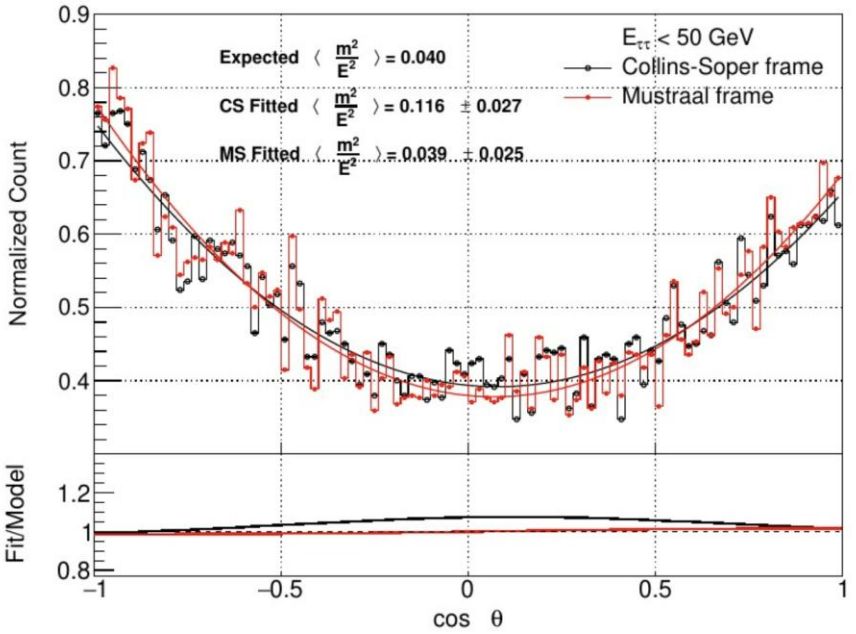

Statistics?

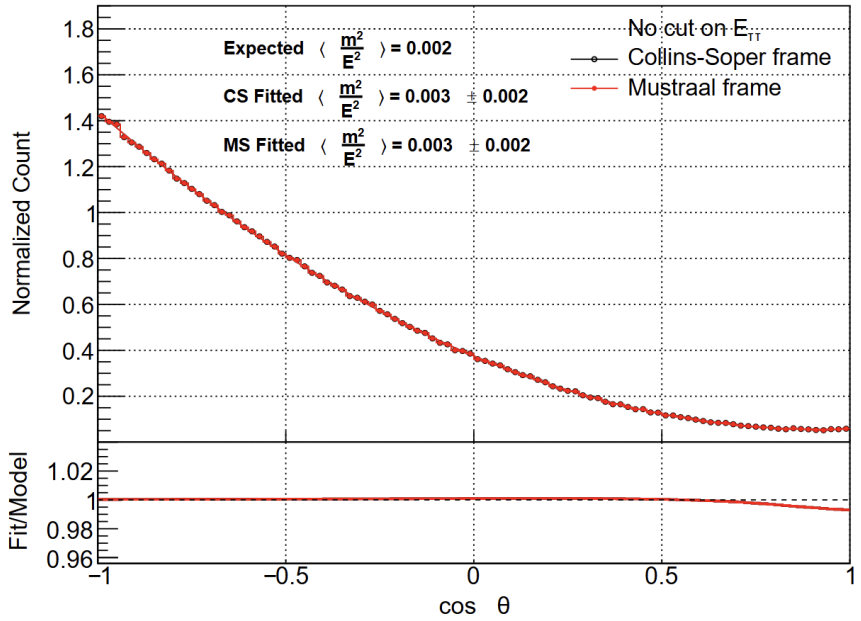

1 Million events

10 Million events

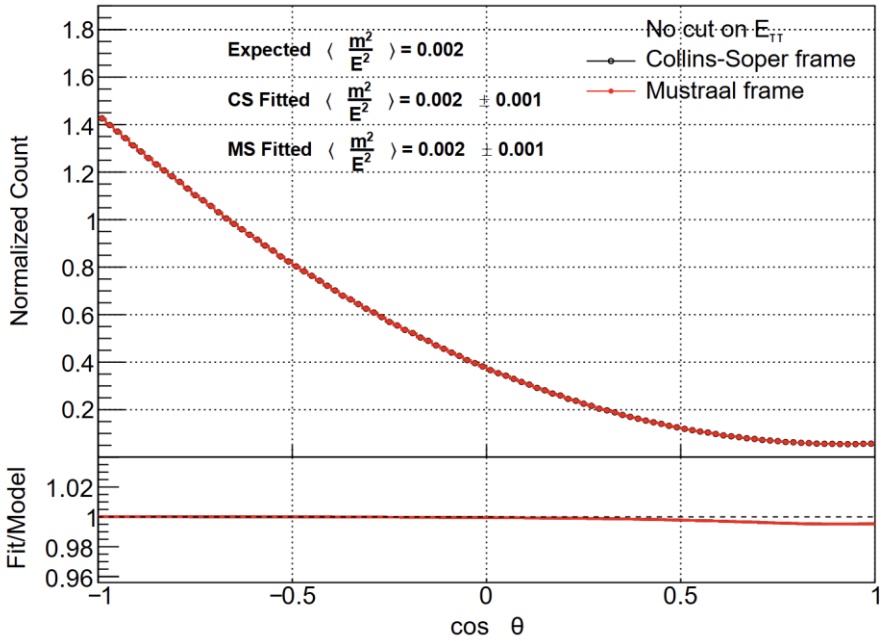

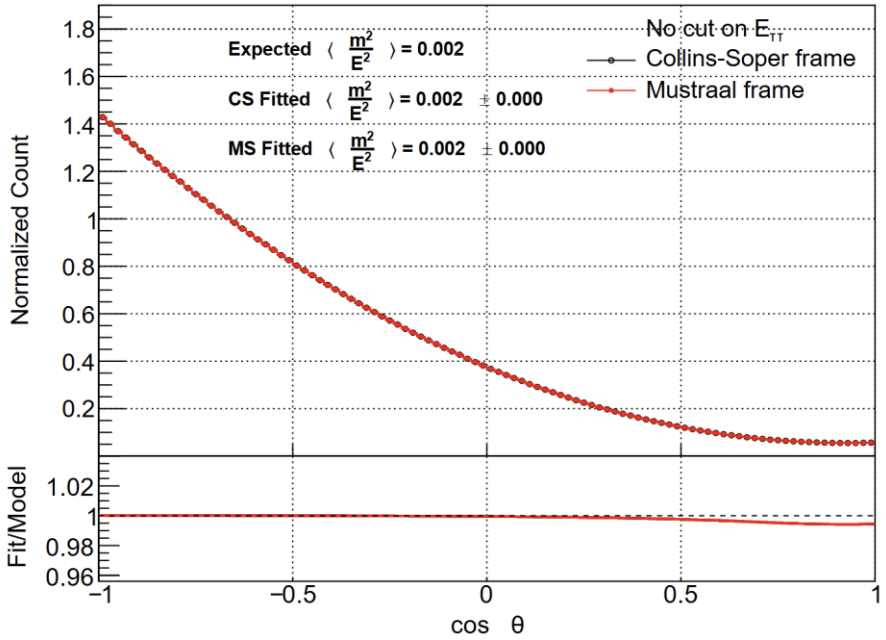

50 Million events

- Present when ISR is not there.
- Statistics probably not the reason and it is clear from large number of events.

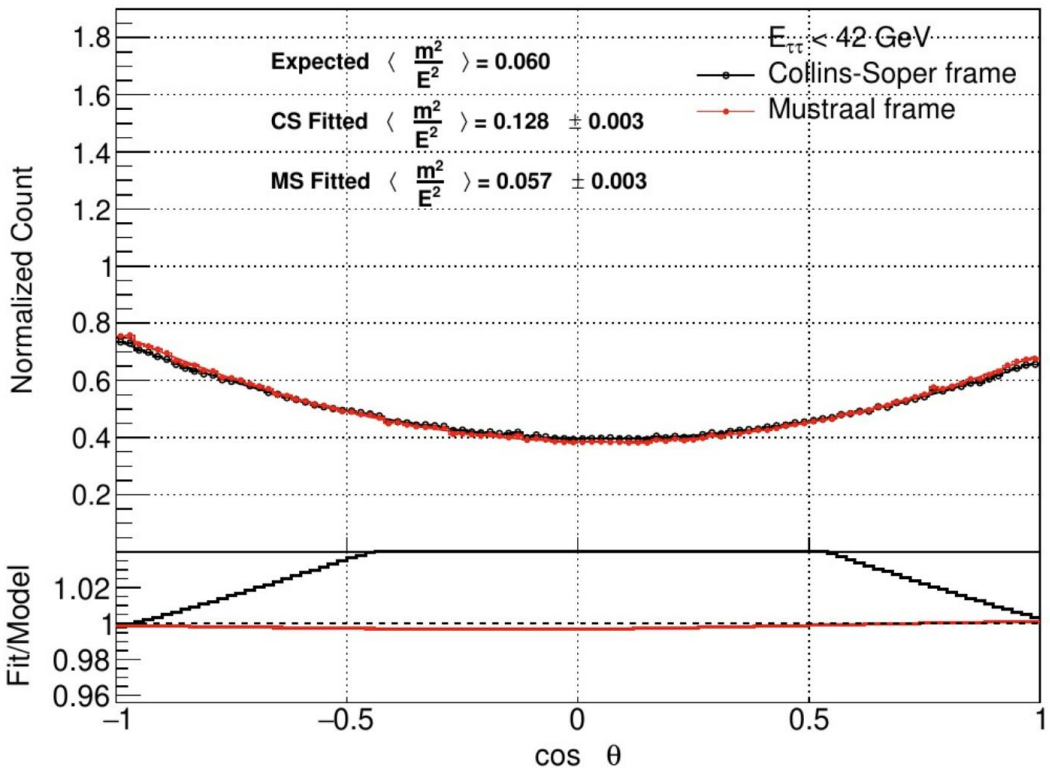
$E_{\tau\tau} < 42$ GeV
Expected $\langle \frac{m^2}{E^2} \rangle = 0.060$
CS Fitted $\langle \frac{m^2}{E^2} \rangle = 0.128 \pm 0.003$
MS Fitted $\langle \frac{m^2}{E^2} \rangle = 0.057 \pm 0.003$
Collins-Soper frame
Mustraal frame
Normalized Count
Fit/Model
cos θ

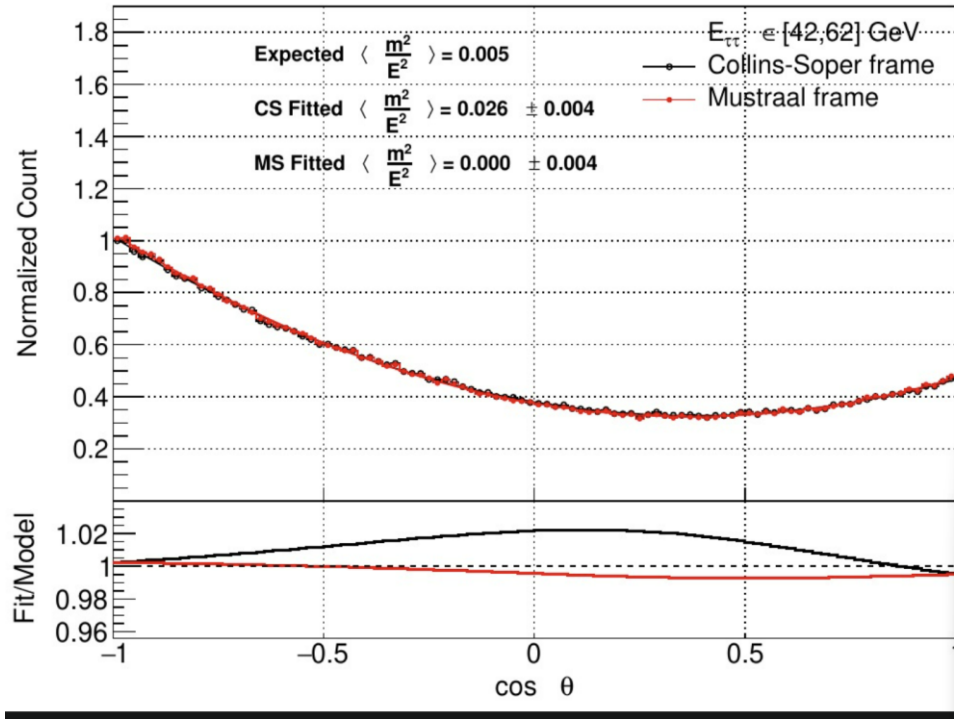
$E_{\tau\tau} \in [42,62]$ GeV
Expected $\langle \frac{m^2}{E^2} \rangle = 0.005$
CS Fitted $\langle \frac{m^2}{E^2} \rangle = 0.026 \pm 0.004$
MS Fitted $\langle \frac{m^2}{E^2} \rangle = 0.000 \pm 0.004$
Collins-Soper frame
Mustraal frame
Normalized Count
Fit/Model
cos θ

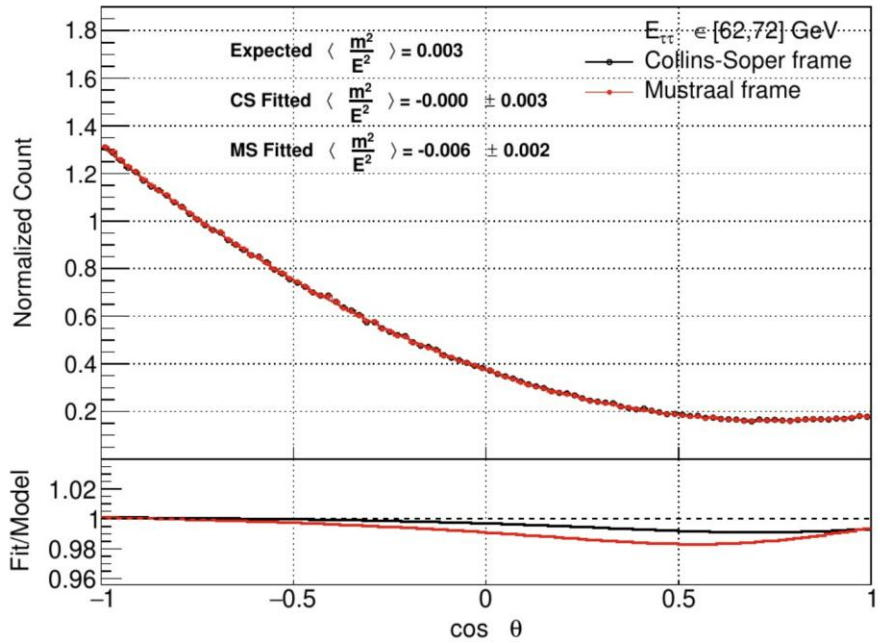
$E_{\tau\tau} \in [62,72]$ GeV
Collins-Soper frame
Mustraal frame
Expected $\langle \frac{m^2}{E^2} \rangle = 0.003$
CS Fitted $\langle \frac{m^2}{E^2} \rangle = -0.000 \pm 0.003$
MS Fitted $\langle \frac{m^2}{E^2} \rangle = -0.006 \pm 0.002$
Normalized Count
Fit/Model
cos θ

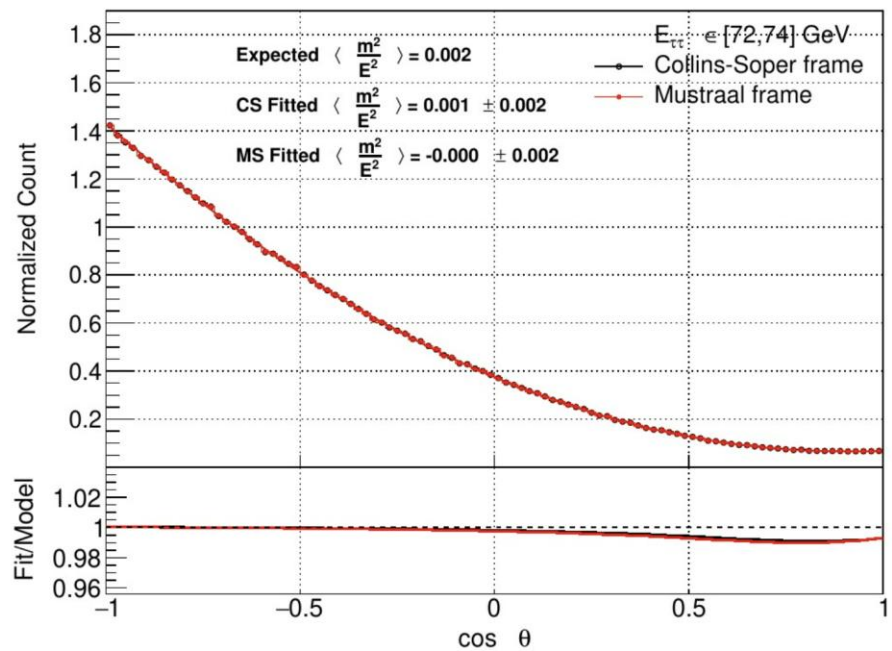
$E_{\tau\tau} \in [72,74]$ GeV
Collins-Soper frame
Mustraal frame
Expected $\langle \frac{m^2}{E^2} \rangle = 0.002$
CS Fitted $\langle \frac{m^2}{E^2} \rangle = 0.001 \pm 0.002$
MS Fitted $\langle \frac{m^2}{E^2} \rangle = -0.000 \pm 0.002$
Normalized Count
Fit/Model
cos θ

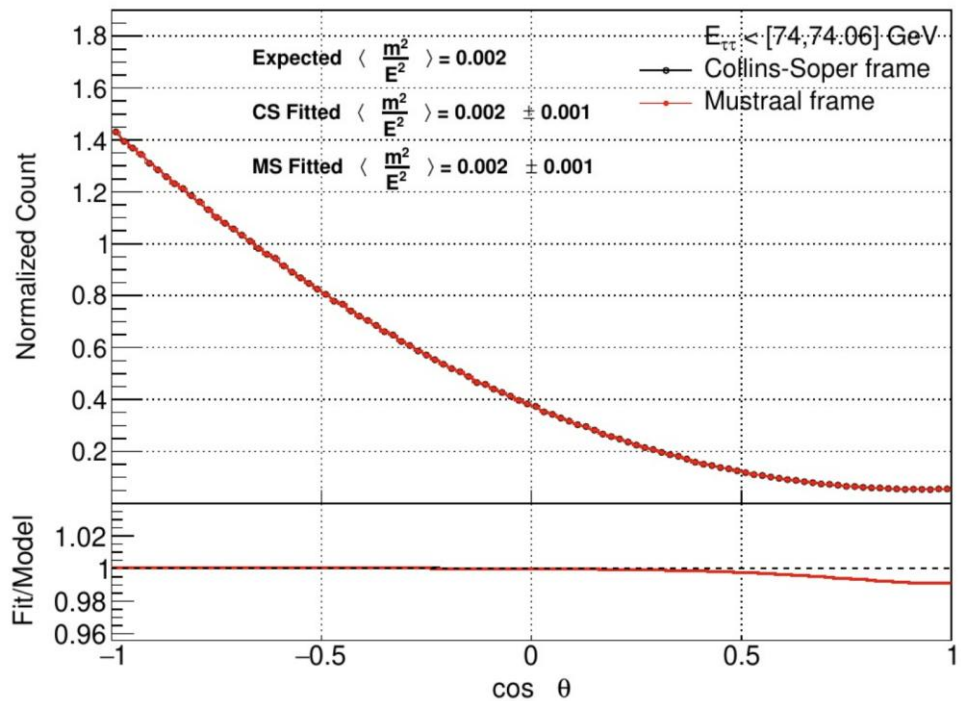
$E_{\tau\tau} \in [74,74.06]$ GeV
Collins-Soper frame
Mustraal frame
Expected $\langle \frac{m^2}{E^2} \rangle = 0.002$
CS Fitted $\langle \frac{m^2}{E^2} \rangle = 0.002 \pm 0.001$
MS Fitted $\langle \frac{m^2}{E^2} \rangle = 0.002 \pm 0.001$
Normalized Count
Fit/Model
cos θ

Electroweak Form Factors:

D. Bardin et al., Comp. Phys. Comun. 133 (2001) 229-395

After some trivial algebra one derives the final expressions:

$$\rho_{ef} = 1+\frac{g^2}{16\pi^2}\left\{-\Delta\rho_z^F+\mathcal{D}_z^F(s)+\frac{5}{3}B_0^F(-s;M_w,M_w)-\frac{9}{4}\frac{c_w^2}{s_w^2}\ln c_w^2-6\right.$$
$$+\frac{5}{8}c_w^2\left(1+c_w^2\right)+\frac{1}{4c_w^2}\left(3v_e^2+a_e^2+3v_f^2+a_f^2\right)\mathcal{F}_z(s)+\hat{\mathcal{F}}_w^0(s)+\hat{\mathcal{F}}_w(s)$$
$$\left.-\frac{r_t}{4}\left[B_0^F(-s;M_w,M_w)+1\right]-c_w^2(R_z-1)s\hat{\mathcal{B}}_{ww}^d(s,t)\right\},$$

$$\kappa_e = 1+\frac{g^2}{16\pi^2}\left\{-\frac{c_w^2}{s_w^2}\Delta\rho^F-\Pi_{z\gamma}^F(s)-\frac{1}{6}B_0^F(-s;M_w,M_w)-\frac{1}{9}-\frac{v_e\sigma_e}{2c_w^2}\mathcal{F}_z(s)\right.$$
$$-\hat{\mathcal{F}}_w^0(s)+(R_z-1)\left[\frac{|Q_f|}{2}\left(1-4|Q_f|s_w^2\right)\mathcal{F}_z(s)+c_w^2\left[\hat{\mathcal{F}}_{w_n}(s)\right.\right.$$
$$\left.\left.-|Q_{f'}|\mathcal{F}_{w_a}(s)+s\hat{\mathcal{B}}_{ww}^d(s,t)\right]\right]\Bigg\},$$

$$\kappa_f = 1+\frac{g^2}{16\pi^2}\left\{-\frac{c_w^2}{s_w^2}\Delta\rho^F-\Pi_{z\gamma}^F(s)-\frac{1}{6}B_0^F(-s;M_w,M_w)-\frac{1}{9}-\frac{v_f\sigma_f}{2c_w^2}\mathcal{F}_z(s)\right.$$
$$-\hat{\mathcal{F}}_w(s)+(R_z-1)\left[\frac{|Q_e|}{2}\left(1-4|Q_e|s_w^2\right)\mathcal{F}_z(s)+c_w^2\left[\hat{\mathcal{F}}_{w_n}^0(s)\right.\right.$$
$$\left.\left.\left.-|Q_{e'}|\mathcal{F}_{w_a}(s)+s\hat{\mathcal{B}}_{ww}^d(s,t)\right]-\frac{r_t}{4}\left[B_0^F(-s;M_w,M_w)+1\right]\right\},$$

Interference

$$\kappa_{ef} = 1+\frac{g^2}{16\pi^2}\left\{-2\frac{c_w^2}{s_w^2}\Delta\rho^F-2\Pi_{z\gamma}^F(s)-\frac{1}{3}B_0^F(-s;M_w,M_w)-\frac{2}{9}\right.$$
$$-\frac{1}{4c_w^2}\left[\frac{\delta_e^2+\delta_f^2}{s_w^2}(R_w-1)+3v_e^2+a_e^2+3v_f^2+a_f^2\right]\mathcal{F}_z(s)$$
$$-\hat{\mathcal{F}}_w^0(s)-\hat{\mathcal{F}}_w(s)-\frac{r_t}{4}\left[B_0^F(-s;M_w,M_w)+1\right]$$
$$\left.+c_w^2(R_z-1)\left[\frac{2}{3}-\hat{\Pi}_{z\gamma}^{\mathrm{bos},F}(s)+s\hat{\mathcal{B}}_{ww}^d(s,t)\right]\right\}.$$

Fermionic loops in γ* propagator

Box

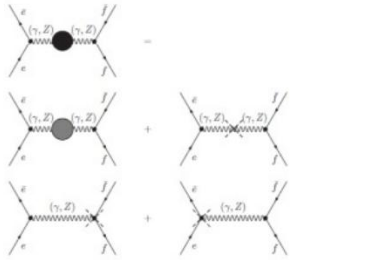

Figure A.11. *Bosonic self-energies and bosonic counter-terms for $e\bar{e}\to(Z,\gamma)\to f\bar{f}$*

Figure A.10. *Electron (a) and final fermion (b) vertices in $e\bar{e}\to(Z)\to f\bar{f}$*

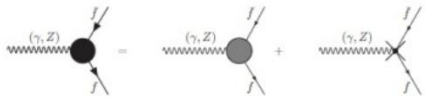

Figure A.6. *Off-shell $Zf\bar{f}$ and $\gamma f\bar{f}$ vertices*

Figure A.7. *The WW boxes*

etc. etc.

Thank you

Helicity attribute of standalone code

$$
\begin{aligned}
V_i^a &= \delta_i^a(\delta_i^t + \delta_i^z) \\
V &= \left[\begin{pmatrix} 1 \\ 0 \\ 0 \\ 0 \end{pmatrix} (1 \quad 0 \quad 0 \quad 0) + \begin{pmatrix} 0 \\ 0 \\ 0 \\ 1 \end{pmatrix} (0 \quad 0 \quad 0 \quad 1) \right] \\
&= \frac{1}{2} \left[\begin{pmatrix} 1 \\ 0 \\ 0 \\ 1 \end{pmatrix} (1 \quad 0 \quad 0 \quad 1) + \begin{pmatrix} 1 \\ 0 \\ 0 \\ -1 \end{pmatrix} (1 \quad 0 \quad 0 \quad -1) \right] \\
&= \frac{1}{2}(s^+ s^{+^T} + s^- s^{-^T}) = \frac{1}{2} \sum_{i=\pm} s^i s^{i^T}
\end{aligned}
$$

$$
\begin{aligned}
wt_{\text{appx}} &= \sum_{i,j,a,b=t,z} h_+^a V_a^i R_{ij} V_b^j h_-^b \\
&= \frac{1}{4} \sum_{i,j,a,b=t,z} h_+^a \sum_{m=\pm} (s^m)_a (s^{m^T})^i R_{ij} \sum_{n=\pm} (s^n)_b (s^{n^T})^j h_-^b \\
&= \frac{1}{4} \sum_{m=\pm} \sum_{n=\pm} \sum_{i,j,a,b=t,z} \left(h_+^a (s^m)_a\right) \left((s^{m^T})^i R_{ij} (s^{n^T})^j\right) \left((s^n)_b h_-^b\right) \\
&= \frac{1}{4} \sum_{m=\pm} \sum_{n=\pm} (h_+ \cdot s^m)(s^m \cdot R \cdot s^n)(h_- \cdot s^n)
\end{aligned}
$$

In tau rest frame : h[0] = 1

$$wt_{appx}(m,n) = (1 + mh_z^+)\,(R_{00} + nR_{03} + mR_{30} + mnR_{33})\,(1 + nh_z^-), \quad m,n = \pm 1$$

Snapshot of hepmc3 event output :

```
E 0 3 10
U GEV MM
W 1.0000000000000000000000e+00 9.941564018963549020924 1e-01 9.999867056880801241547 4e-01 1.0000000000000000000000e+00
A 0 GenCrossSection 1.19754436e+03 0.00000000e+00 -1 -1 1.19054639e+03 0.00000000e+00 1.19752844e+03 0.00000000e+00 1.19754436e+03 0.00000000e+00
A 0 SpinWT 0.988999
A 0 SpinWThelApprox 1.12984
A 3 approximateHelicity 1
A 4 approximateHelicity -1
A 3 polarimetricInLabFrame 0.291323 0.776381 4.414030 4.491247
A 4 polarimetricInLabFrame 0.407648 -1.428345 -2.695083 3.077307
P 1 0 11 0.0000000000000000e+00 0.0000000000000000e+00 5.2899999753194660e+00 5.2900000000000000e+00 5.1099907047554905e-04 4
P 2 0 -11 0.0000000000000000e+00 0.0000000000000000e+00 -5.2899999753194660e+00 5.2900000000000000e+00 5.1099907047554905e-04 4
V -1 0 [1,2]
P 3 -1 15 8.0337335211367777e-01 1.6251771340373224e+00 4.6410757198752819e+00 5.2900000000000000e+00 1.7770500000000009e+00 2
P 4 -1 -15 -8.0337335211367777e-01 -1.6251771340373224e+00 -4.6410757198752819e+00 5.2900000000000000e+00 1.7770500000000009e+00 2
P 5 3 16 7.0796132087707520e-01 1.5019812583923340e+00 2.5320308208465576e+00 3.0279262065887451e+00 0.0000000000000000e+00 1
P 6 3 -211 7.3834755457937717e-03 3.0162120237946510e-02 2.0661890506744385e+00 2.0711305141448975e+00 1.3957128747269865e-01 1
P 7 3 111 8.8028505444526672e-02 9.3033641576766968e-02 4.2855702340602875e-02 1.9094325602054596e-01 1.3497569988998021e-01 1
P 8 4 -16 1.4564158022403717e-01 -8.5076844692230225e-01 -3.0528807640075684e+00 3.1725540161132812e+00 0.0000000000000000e+00 1
P 9 4 211 -4.4488441199064255e-02 -3.6534217000007629e-01 -3.7024828791618347e-01 5.4038661718368530e-01 1.3956997795254725e-01 1
P 10 4 111 -9.0452653169631958e-01 -4.0906661748886108e-01 -1.2179472446441650e+00 1.5770598649978638e+00 1.3497623110909371e-01 1
```

New version of KKMC can be found here: https://holeczek.web.cern.ch/public/KrakowHEPSoft/KKMCee-dev/

- With CM energy 150 GeV.

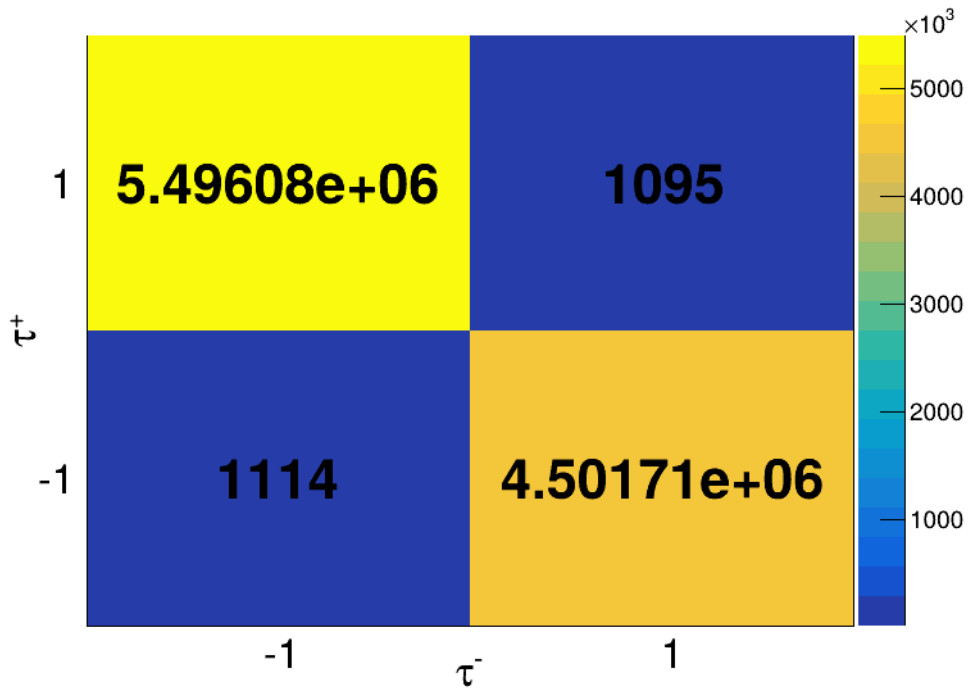

Our code

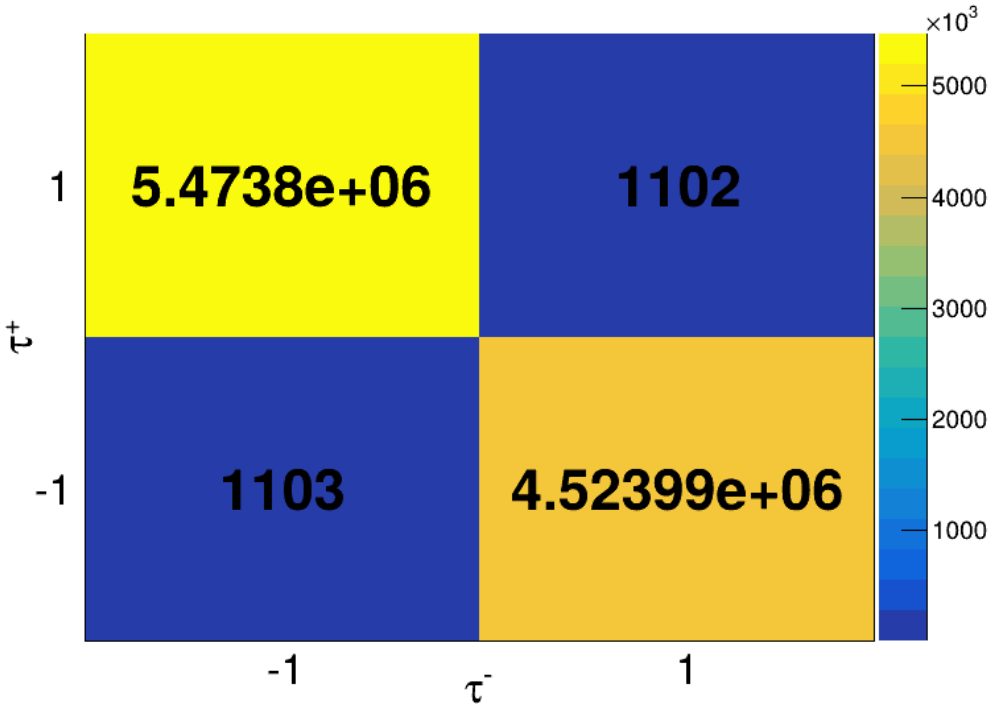

KKMCee

Conclusion

1. Belle II: expected reach for τ EDM:
$\left|d_{\backslash \mathrm{tau}}\right| < 10\text{^}\{-18\}$ e·cm with full statistics.

2. FCC-ee or SuperKEKB upgrades could probe one order of magnitude deeper.

3. Its modulation phase is a **direct window into CP-violating τ dynamics** — a precision tool for the next generation of collider experiments.

4. The **helicity fractions (τ_L, τ_R)** can be reconstructed externally — validated against KKMC with …….suprecision.

5. This allows **event-by-event helicity assignment**, reproducing the ALEPH strategy at the Z pole.

6. My talk can be understood as addressing the question of factorisation quality for spin-dependent quantities. Thus still coincide with conference subject.

Introduction

- Collider experiments reach per-mille precision
  LHC, Belle II, FCC-ee → require control of QED effects at **0.1% level**.

- Photon emission (bremsstrahlung) modifies observables, acceptance details, signal/background separation
  Shift-invariant mass peaks (Z, W).
  Alters angular distributions, acoplanarity.
  Affects extracted couplings and branching ratios.

- Theory challenge
  Soft/collinear photons → **divergences**. Beware of detector response.
  Real-virtual corrections, partial cancellation (KLN theorem), make observables finite.
  Monte Carlo must implement this **event by event**, not only analytically for global quantities.

- Need for tools like KKMC(excl. exp. + $\alpha, \mathrm{O}\left(\alpha^2 L\right)$) and PHOTOS (excl. exp. + O (α))
  Provide a precision simulation of radiative corrections in realistic detector conditions.
  Essential for reliable interpretation of experimental data.

Mustraal Frame(Soft photon):

- The differential cross section corrected for virtual corrections and soft bremsstrahlung up to an energy is given by,

$$\frac{d\sigma'}{d\Omega} = \frac{\alpha^2}{4s}\left[(1+c^2)f'(s) + cg'(s) + \delta(s,\theta)\right].$$

- No need for reconstruction of beam axis:

  pb1 = (E,0,0,E)

  pb2 = (E,0,0,-E)

- Other input from hepmc3 (1→ + , 2 → -):

  p1 =

  p2=

  h1, h2, decay products (including neutrinos ?)

- 1st selection: Rotation to lepton-pair rest frame,

  p1, p2 are back to back but not pb1, pb2.

- Z1 = pb1 – pb2

  Z2 = pb2 – pb1

- Define the angle θ :

  cos θ1 = Angle (p1 , Z1)

  cos θ2 = Angle (p1, Z2)

  } Stochastic choice here!!

- Probability of choice: $P_{\pm} = \frac{1}{2}(1 \pm g'/2f').$

Properties enabling kkmc associated application:

- This is of interest: (i) people want to use it and (ii) **I need to learn** .
- We prepare the user-friendly external code for practical applications such as:

  Helicity-like flags (e.g. for g_V/g_A fits) ,

  Tau polarimetric vectors (e.g. for New Physics searches),

ADVANTAGE: The user does not need to know the technicalities and details of frame orientations of KKMCee.
User need to worry about own choice
of reference frames only, and assure their relation to lab frame.

Preparation of External to kkmc application:

- Our ongoing work is to prepare the user-friendly external code that can be used for practical applications such as,

  Helicity-like flags

  New physics searches

ADVANTAGE: The user does not need to know the technicalities and details of frame orientations of KKMCee.
User need to worry about their choice
of reference frames only and their relation to lab frame.

- For now, two choices of reference frames are used in application for factorized-out Born configuration:
- a) Colins-Soper frame b) Mustraal frame

SHORT INTRODUCTION ON PHOTOS

- The PHOTOS Monte Carlo[E. Barberio, B. van Eijk, and Z. Was, Comput. Phys. Commun. 66(1991) 115-128, E. Barberio and Z. Was, Comput. Phys. Commun. 79 (1994) 291-308, P. Golonka and Z. Was, Eur. Phys. J. C50 (2007) 53-62] is a universal Monte Carlo algorithm that is designed for simulating QED radiative corrections in decays of particles and resonances.
- The program has two steps,

a) The exact multiphoton phase space starting from a **Poissonian distribution**, while the matrix element is approximately taken as a process-independent multidimensional kernel, with no phase space constraints.

b) Iteratively, phase space constraints and matrix elements are introduced.

c) The same emission kernel can be used in a mode where maximum photon multiplicity is fixed to 1 or 2. This operation mode is prepared for tests and comparisons with fixed order matrix element calculations.

- Controlled by ME_channel:

  0 → MEC **off** (default soft kernel only).

  1 → MEC **on for Z decays** ,$Z \to \ell^+\ell^-\gamma$

  2 → MEC **on for W decays** ($W \to \ell\nu\gamma$).

Effect:

ME_channel=0: Universal kernel, precise at **~0.3%**, but less accurate in rare hard-photon corners.

ME_channel=1/2: Exact $O(\alpha)$matrix element (YFS β_1) applied to all photons.

KKMCee

- **Previous talks: Scott Yost, B.F.L. Ward, *Zbigniew Andrzej Was***
- Purpose
  - High-precision generator for $e^+e^- \to f\bar{f}$ processes.
  - Includes both **initial-state radiation (ISR)** and **final-state radiation (FSR) and interference**.
  - Developed for LEP, Belle-II, FCC-ee precision needs.
- Algorithm basics
  - Based on **Yennie–Frautschi–Suura (YFS) exclusive exponentiation**.
  - **All-orders photons** (eikonal parts of ME only) explicitly generated → IR-safe.
  - QED Exact $\mathcal{O}(\alpha^2)$**matrix elements** included (through reweighting) as YFS β_1 , β_2 corrections to ME
  - ISR–FSR **interference** consistently implemented.
  - Multi-photon phase space generation uses **conformal symmetry mapping**.
- Precision

  Designed and validated for **per-mille (0.1%) or better** accuracy.

  Used in LEP precision electroweak fits.

  Hopefully framework ready for $\mathcal{O}(\alpha^3)$ extension and precision 0.01%.
- Current version of KKMcee is available at https://holeczek.web.cern.ch/public/KrakowHEPSoft/KKMCee-dev/
- This is long project and many intermediate solutions helpful for tests are needed. Also, for daily research.